



# Chemically deposited $\text{In}_2\text{S}_3$ – $\text{Ag}_2\text{S}$ layers to obtain $\text{AgInS}_2$ thin films by thermal annealing

S. Lugo<sup>a</sup>, Y. Peña<sup>a,\*</sup>, M. Calixto-Rodriguez<sup>b</sup>, C. López-Mata<sup>c</sup>, M.L. Ramón<sup>b</sup>, I. Gómez<sup>a</sup>, A. Acosta<sup>a</sup>

<sup>a</sup> Universidad Autónoma de Nuevo León, UANL, Fac. de Ciencias Químicas, Av. Universidad S/N Ciudad Universitaria San Nicolás de los Garza Nuevo León, C.P. 66451 Mexico

<sup>b</sup> Centro de Investigación en Energía-Universidad Nacional Autónoma de México, 62580, Temixco, Morelos, Mexico

<sup>c</sup> Instituto Tecnológico de Chetumal, Av. Insurgentes No. 330, C.P. 77013, Col. David Gustavo Gtz., Chetumal, Quintana Roo, Mexico

## ARTICLE INFO

### Article history:

Received 9 February 2012

Received in revised form 1 September 2012

Accepted 16 September 2012

Available online 24 September 2012

### Keywords:

Silver indium sulfide

Thin films

Chemical bath deposition

## ABSTRACT

$\text{AgInS}_2$  thin films were obtained by the annealing of chemical bath deposited  $\text{In}_2\text{S}_3$ – $\text{Ag}_2\text{S}$  layers at 400 °C in  $\text{N}_2$  for 1 h. According to the XRD and EDX results the chalcopyrite structure of  $\text{AgInS}_2$  has been obtained. These films have an optical band gap,  $E_g$ , of 1.86 eV and an electrical conductivity value of  $1.2 \times 10^{-3} (\Omega \text{ cm})^{-1}$ .

© 2012 Elsevier B.V. All rights reserved.

## 1. Introduction

The  $\text{AgInS}_2$  compound can be grown as tetragonal and orthorhombic phase [1]. In the tetragonal crystal structure it shows two direct band gaps, at 1.86 and 2.02 eV [1], while in the orthorhombic crystal structure it shows two band gaps at 1.96 and 2.04 eV [2].  $\text{AgInS}_2$  belongs to the I–III–VI<sub>2</sub> group. It is one of the least studied materials compared to the thorough investigated copper indium chalcogenides (CIS) used in photovoltaic device applications [2,3]. For example, making a comparison between  $\text{CuInS}_2$  and  $\text{AgInS}_2$  we have found out that  $\text{CuInS}_2$  has an optical band gap of 1.5 eV while  $\text{AgInS}_2$  has a wider band gap (1.86–2.04 eV); both materials have a high absorption coefficient;  $\text{CuInS}_2$  shows a p-type electrical conductivity, and although  $\text{AgInS}_2$  shows a n-type electrical conductivity [4], it can be doped with Sb [5] and Sn [6] atoms to change its conductivity to p-type.

Several methods such as thermal evaporation [7], spray pyrolysis [8], co-evaporation [9], and chemical bath deposition (CBD) [10] have been used to obtain  $\text{AgInS}_2$  thin films, but CBD has proved to be the most attractive, easy to apply, less expensive and suitable for large area deposition. Moreover, in comparison with thermal evaporation and co-evaporation methods CBD does not require high vacuum systems.

In this work, the results of the structural, chemical composition, optical and electrical characterization of the polycrystalline silver indium sulfide thin films obtained through the annealing of chemically deposited  $\text{In}_2\text{S}_3$ – $\text{Ag}_2\text{S}$  layers are presented.

## 2. Experimental details

### 2.1. Deposition of $\text{In}_2\text{S}_3$ thin films

$\text{In}_2\text{S}_3$  thin films were deposited by chemical bath deposition method using a mixture of the following reagents in the order described here: 10 mL of  $\text{In}(\text{NO}_3)_3$  0.1 M, 2 mL of  $\text{CH}_3\text{COOH}$  0.1 M, 16 mL of  $\text{CH}_3\text{CSNH}_2$  1 M, and water to complete a volume of 100 mL. The glass substrates (Corning, 25 mm × 75 mm) were placed vertically in the solution. The chemical deposition was carried out at 35 °C for 22 h, since lower deposition temperature produces thinner films, and higher deposition temperature accelerates the precipitation of the solution resulting in films of low quality.

### 2.2. Deposition of $\text{Ag}_2\text{S}$ thin films

Chemically deposited silver sulfide thin films were obtained by following the procedure given in Ref. [11] using: 12.5 mL of 0.1 M solution of  $\text{AgNO}_3$ , 4.5 mL of 1 M solution of  $\text{Na}_2\text{S}_2\text{O}_3$ , 5 mL of 0.5 M solution of  $\text{C}_3\text{H}_8\text{N}_2\text{S}$  in the given sequence then adding deionized water while stirring the solution until completing a 100 mL volume. Indium sulfide thin films prepared previously were used as

\* Corresponding author. Tel.: +52 8183294000x6363/8183294010; fax: +52 8183765375.

E-mail address: [yolapm@gmail.com](mailto:yolapm@gmail.com) (Y. Peña).

substrates. The substrates were placed vertically in the solution at 35 °C for 1, 2 or 3 h. For this study we chose a deposition time of 1 h.

### 2.3. Thermal annealing

The thin films of  $\text{In}_2\text{S}_3\text{-Ag}_2\text{S}$  were thermally annealed in a tubular furnace (Thermolyne 21100). We have made some annealing experiments of the  $\text{In}_2\text{S}_3/\text{Ag}_2\text{S}$  layers at 350 °C for 60 min and at 400 °C for 60 and 90 min in  $\text{N}_2$  atmosphere. For this study we chose an annealing temperature and time of 400 °C and 60 min in order for it to react and convert the  $\text{In}_2\text{S}_3\text{-Ag}_2\text{S}$  films into  $\text{AgInS}_2$ .

### 2.4. Characterization

X-ray diffraction (XRD) patterns were recorded on a Rigaku D-Max 2000 diffractometer using  $\text{Cu K}\alpha$  radiation ( $\lambda = 1.5406 \text{ \AA}$ ). The chemical composition of the annealed films was determined by energy dispersive X-ray spectroscopy (EDX) using an Inca Oxford Instruments system attached to the scanning electron microscope. The surface morphology was studied by scanning electron microscopy (SEM) JEOL model JSM 5800LV at 1 kV and 25,000 $\times$ . Field emission atomic force microscopy (FE-AFM) analysis was done using a JEOL JSM-6701 F equipment, the thickness of the film was measured by AFM and SEM. The optical transmittance at normal incidence,  $T(\lambda)$ , and specular reflectance spectra,  $R(\lambda)$ , of the films were measured with a spectrophotometer Shimadzu model UV-1800 in the UV–vis–NIR region (190–1100 nm wavelength range). Hall measurements were recorded to obtain the value and type of the electrical conductivity. The temperature dependent conductivity measurements were performed using equipment named Janis CCS 400/202 N with a temperature range of 300–10 K, and in order to do this it was necessary to apply a pair of coplanar carbon paint electrodes.

## 3. Results and discussion

### 3.1. Structural characterization and chemical compositional analysis

The  $\text{AgInS}_2$  films were obtained by the deposition in sequence of layers of  $\text{Ag}_2\text{S}$ , deposited at 35 °C for 1 h, over an  $\text{In}_2\text{S}_3$  film previously deposited at 35 °C for 22 h. When we performed the annealing of the structure  $\text{In}_2\text{S}_3/\text{Ag}_2\text{S}$  using a  $\text{Ag}_2\text{S}$  layer deposited for 2 or 3 h, the XRD results showed that the film has a mixture of phases:  $\text{AgInS}_2$  (tetragonal and orthorhombic) and  $\text{Ag}_2\text{S}$  (acanthite).

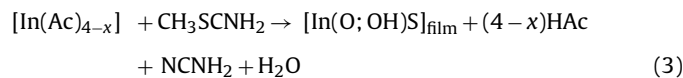
When we made the annealing experiments of the  $\text{In}_2\text{S}_3/\text{Ag}_2\text{S}$  layers at 400 °C for 60 and 90 min we found from the XRD results that there is no difference between the annealing time considered at 60 and 90 min. When we performed the annealing of the  $\text{In}_2\text{S}_3/\text{Ag}_2\text{S}$  layers at 350 °C, we found out a mixture of phases ( $\text{In}_2\text{S}_3$  and  $\text{AgInS}_2$ ), not just the one which corresponds to the  $\text{AgInS}_2$ . In addition, the XRD results showed that  $\text{AgInS}_2$  film has not crystallized completely at 350 °C. So, this was the reason, we decided to perform the annealing of the structure  $\text{In}_2\text{S}_3/\text{Ag}_2\text{S}$  at 400 °C for 1 h.

The chemical reactions for the formation of  $\text{AgInS}_2$  are described below:

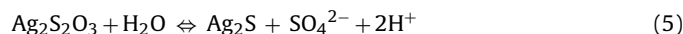
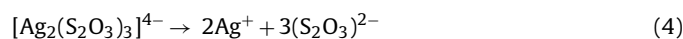
The presence of the air in the solution environment favoured the production of oxide at a lower deposition temperature (35 °C). There are two possibilities proposed to explain the formation of  $\text{In}_2\text{O}_3$  from the thioacetamide–In(III) solution. On one hand, the precipitation of the hydroxide [12]:



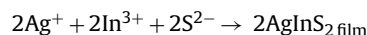
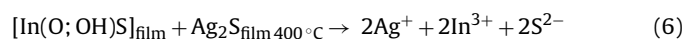
A second route can be proposed for the deposition of thin films of  $\text{In}(\text{O};\text{OH})\text{S}$ , thioacetamide was used as source of  $\text{S}^{2-}$  through the hydrolysis in an acidic environment; and acetic acid ( $\text{AcOH}$ ) was used as complexing agent; the entire reaction can be written as follows [13]:



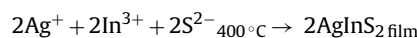
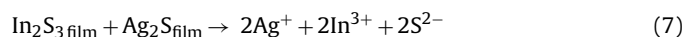
The chemical reactions for the deposition of  $\text{Ag}_2\text{S}$  films taking place in the chemical bath could be considered as below. Silver ions,  $\text{Ag}^+$ , in the bath combine with  $\text{S}_2\text{O}_3^{2-}$  to initially form an insoluble  $\text{Ag}_2\text{S}_2\text{O}_3$ , which in excess of  $\text{S}_2\text{O}_3^{2-}$ , form soluble complexes:



The overall reaction of the ternary system films containing the  $\text{AgInS}_2$  phase is given by:



or



From the XRD pattern of the sample it was found that the ternary system contains the  $\text{AgInS}_2$  phase (see Fig. 1), which is in agreement with literature [14]. The XRD pattern shown in Fig. 1 corresponds to both structures of  $\text{AgInS}_2$ : the tetragonal (chalcopyrite) structure of  $\text{AgInS}_2$  T(JCPDS 25-1330) with reflections in (1 1 2), (2 0 0), (2 2 0), (2 0 4), and (3 1 2); and the orthorhombic structure of  $\text{AgInS}_2$  O(JCPDS 25-1328) with reflections in (2 0 0), (0 0 2), (1 2 1), (0 4 0), (3 2 0), and (0 4 2). Additionally, Fig. 1 shows two peaks (2 2 2) and (6 2 2) which correspond to indium oxide ( $\text{In}_2\text{O}_3$ ).

From the chemical compositional analysis we found the following results  $\text{Ag} = 22.21 \text{ at\%}$ ,  $\text{In} = 29.52 \text{ at\%}$ , and  $\text{S} = 48.27 \text{ at\%}$ . The error margin in EDX data is 5%. These results showed that the composition of the film is close to the stoichiometric composition of  $\text{AgInS}_2$ .

### 3.2. SEM and AFM measurements

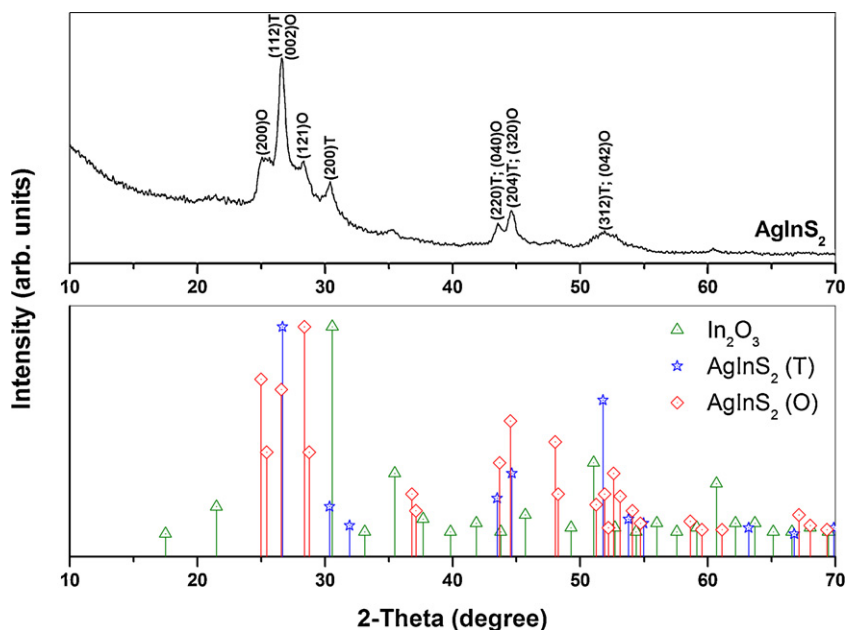
Fig. 2(a) shows a typical SEM image of the morphology of the  $\text{In}_2\text{S}_3\text{-Ag}_2\text{S}$  samples, measured after the films reacted thermally in  $\text{N}_2$  at 400 °C for 1 h. In this picture we can see that there are clusters of quasi-spherical shape of varying sizes. Fig. 2(c) shows a cross sectional SEM image of the same  $\text{In}_2\text{S}_3\text{-Ag}_2\text{S}$  sample. In this picture we can see that the film thickness is in the order of 200 nm.

Fig. 2(b) shows a typical AFM image of the surface topography in 3D of the  $\text{In}_2\text{S}_3\text{-Ag}_2\text{S}$  samples. This film shows that after the thermal annealing small grains had coalesced, resulting in bigger grains on the film surface. The average film thickness was 270 nm for the resulting  $\text{AgInS}_2$  film.

### 3.3. Optical and electrical characterization

Optical transmission,  $T(\lambda)$ , and reflection spectra,  $R(\lambda)$ , were recorded in the range of 300–1100 nm. Fig. 3 shows  $T(\lambda)$  and  $R(\lambda)$  responses for  $\text{AgInS}_2$  film. The absorption coefficient ( $\alpha$ ) was calculated using  $T(\lambda)$  and  $R(\lambda)$  data and the well known expression, for direct optical transitions [15,16], given by

$$\alpha h\nu = A(h\nu - E_g)^r \quad (1)$$



**Fig. 1.** X-ray diffraction pattern for AgInS<sub>2</sub> film (after annealing the In<sub>2</sub>S<sub>3</sub>–Ag<sub>2</sub>S sample in N<sub>2</sub> at 400 °C for 1 h). “T” corresponds to the tetragonal (chalcopyrite) structure and “O” to the orthorhombic structure of the AgInS<sub>2</sub>.

where  $A$  is a constant, and  $E_g$  is the optical band gap. In this equation  $r = 1/2$  for direct allowed optical transitions and  $3/2$  for the direct forbidden ones. The band-gap value can be obtained from the best linear approximation in the  $(\alpha h\nu)^{1/r}$  vs.  $h\nu$  plot and its extrapolation to  $(\alpha h\nu)^{1/r} = 0$ . Fig. 4 shows the  $(\alpha h\nu)^2$  vs.  $h\nu$  plot for AgInS<sub>2</sub> film. The band gap value obtained was  $E_g = 1.86$  eV, this value agrees with what was reported for chalcopyrite AgInS<sub>2</sub> ( $E_g = 1.87$  eV) [17].

The value of the electrical conductivity for AgInS<sub>2</sub> thin film was  $1.2 \times 10^{-3} (\Omega \text{ cm})^{-1}$ . Hall measurements indicated that the AgInS<sub>2</sub> film has n-type electrical conductivity.

The temperature dependent conductivity measurements were carried out (see Fig. 5). The conductivity is given by Ref. [18]:

$$\sigma = \sigma_1 \exp\left(\frac{-E_a}{KT}\right)$$

where  $\sigma_1$  is the pre-exponential factor proportional to the grain size;  $E_a$  is the activation energy,  $K$  the Boltzmann constant, and  $T$  the temperature in Kelvin. From this equation and the data given

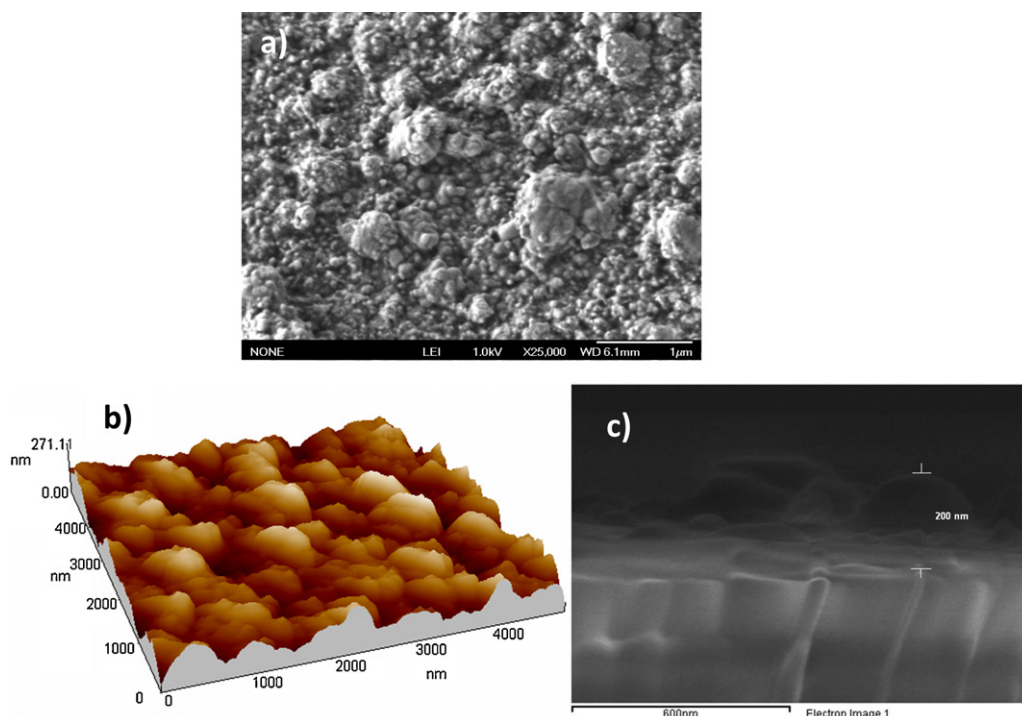


**Fig. 2.** (a) SEM, (b) AFM, and (c) cross sectional SEM images for AgInS<sub>2</sub> film (after annealing the In<sub>2</sub>S<sub>3</sub>–Ag<sub>2</sub>S samples in N<sub>2</sub> at 400 °C for 1 h).

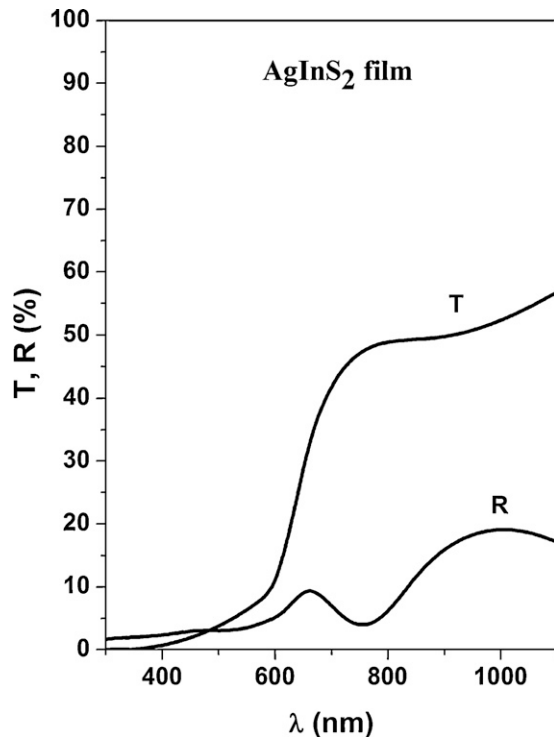


Fig. 3.  $T(\lambda)$  and  $R(\lambda)$  spectra for  $\text{AgInS}_2$  films (after annealing the  $\text{In}_2\text{S}_3\text{-Ag}_2\text{S}$  samples in  $\text{N}_2$  at  $400^\circ\text{C}$  for 1 h).

in Fig. 5 we can calculate the activation energy in a given range of temperature. The above equation becomes to:

$$\ln \sigma = \ln \sigma_1 - \frac{E_a}{KT}$$

Calculating the slop in the plot we can determine the activation energy of the film for different ranges of temperature. From

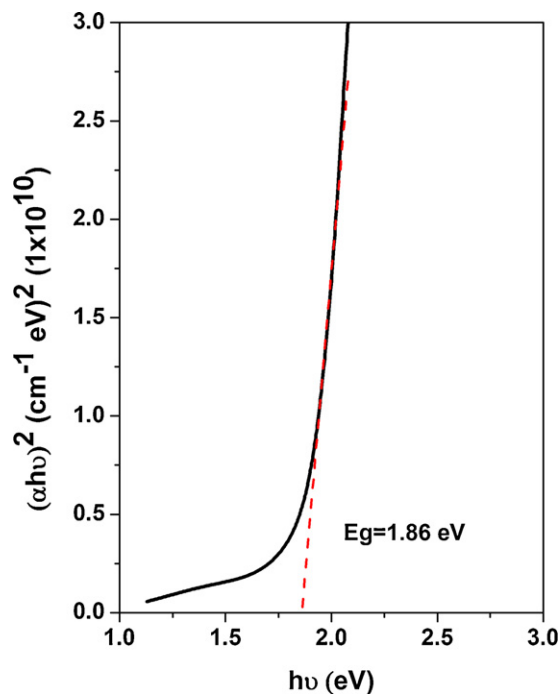


Fig. 4. Plot of  $(\alpha hv)^2$  vs.  $hv$  for  $\text{AgInS}_2$  film (after annealing the  $\text{In}_2\text{S}_3\text{-Ag}_2\text{S}$  sample in  $\text{N}_2$  at  $400^\circ\text{C}$  for 1 h).

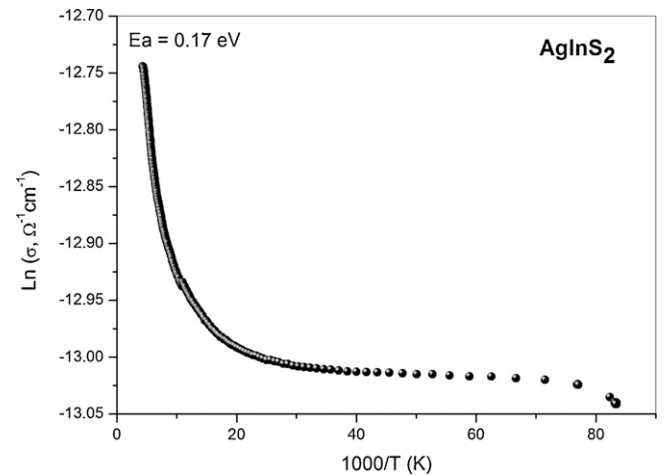


Fig. 5. Temperature dependent conductivity plot for  $\text{AgInS}_2$  film (after annealing the  $\text{In}_2\text{S}_3\text{-Ag}_2\text{S}$  sample in  $\text{N}_2$  at  $400^\circ\text{C}$  for 1 h).

Fig. 5 we can see that semiconducting behavior of the sample is demonstrated. The activation energy ( $E_a$ ) was determined for a temperature range of 290–283 K and 166–220 K being 0.17 eV and 5 meV, respectively.

#### 4. Conclusions

We have reported the results of the structural, morphological, optical, and electrical characterizations of  $\text{AgInS}_2$  thin films obtained by annealing the chemically deposited  $\text{In}_2\text{S}_3\text{-Ag}_2\text{S}$  layers. According to the XRD and EDX results, heating  $\text{In}_2\text{S}_3\text{-Ag}_2\text{S}$  layers at  $400^\circ\text{C}$  in  $\text{N}_2$  for 1 h, the chalcopyrite structure of  $\text{AgInS}_2$  can be obtained. This film has an optical band gap,  $E_g$ , of 1.86 eV and an electrical conductivity value of  $1.2 \times 10^{-3} (\Omega \text{ cm})^{-1}$ . The obtained  $\text{AgInS}_2$  films are suitable for solar cell applications (as a possible buffer layer).

#### Acknowledgements

This work was supported by PAICYT-UANL 2010 (México) grant of Dra. Y. Peña. Technical assistance of Hugo Salas (Laboratorio de Caracterización Microestructural de Materiales Avanzados-UANL) with FE-SEM measurements, and José Campos (CIE-UNAM) with temperature dependent conductivity measurements, which are strongly appreciated.

#### References

- [1] J.L. Shay, B. Tell, L.M. Schiavone, H.M. Kasper, F. Thiel, *Physical Review B* 9 (1974) 1719–1723.
- [2] J.L. Shay, J.H. Wernick, *Ternary Chalcopyrite Semiconductors: Growth, Electronic Properties, and Applications*, Pergamon Press, USA, 1975.
- [3] R.W. Birkmire, *Proc. 26th IEEE PVSC*, Anaheim, CA, 1997, p. 295.
- [4] K. Okamoto, K. Kinoshita, *Solid-State Electronics* 19 (1976) 31–35.
- [5] K. Yoshino, H. Komaki, T. Kakeno, Y. Akaki, T. Ikari, *Journal of Physics and Chemistry of Solids* 64 (2003) 1839–1842.
- [6] M.L. Albor-Aguilera, D. Ramírez-Rosales, M.A. González-Trujillo, *Thin Solid Films* 517 (2009) 2535–2537.
- [7] Y. Akaki, S. Kurihara, M. Shirahama, K. Tsurugida, T. Kakeno, K. Yoshino, *Journal of Materials Science: Materials in Electronics* 16 (7) (2005) 393–396.
- [8] M. Calixto-Rodríguez, H. Martínez, M.E. Calixto, Y. Peña, D. Martínez-Escobar, A. Tiburcio-Silver, A. Sanchez-Juarez, *Materials Science and Engineering B* 174 (2010) 253–256.
- [9] C.A. Arredondo, J. Clavijo, G. Gordillo, *Journal of Physics: Conference Series* 167 (2009) 012050.
- [10] L. Li-Hau, W. Ching-Chen, L. Chia-Hung, L. Tai-Chou, *Chemistry of Materials* 20 (2008) 4475–4483.
- [11] A. Núñez, M.T.S. Nair, P.K. Nair, *Semiconductor Science and Technology* 20 (6) (2005) 576–585.

- [12] B. Asenjo, A.M. Chaparro, M.T. Gutiérrez, J. Herrero, C. Maffiotte, *Electrochimica Acta* 49 (2004) 737–744.
- [13] W. Vallejo, C. Quiñones, G. Gordillo, *Journal of Physics and Chemistry of Solids* 72 (2012) 573–578.
- [14] Ch. Kong-Wei, H. Chao-Ming, P. Guan-Ting, Ch. Wen-Sheng, L. Tai-Chou, C.K.Y. Thomas, *Journal of Photochemistry and Photobiology A: Chemistry* 190 (2007) 77–87.
- [15] T.S. Moss, *Optical Properties of Semiconductors*, Butterworths, London, UK, 1959.
- [16] K.L. Chopra, S.R. Das, *Thin Film Solar Cells*, Plenum Press, New York, 1983.
- [17] M. Ortega-López, A. Morales-Acevedo, O. Solorza-Feria, *Thin Solid Films* 385 (2001) 120–125.
- [18] R. Caballero, C. Guillén, *Thin Solid Films* 431–432 (2003) 200–204.